fluids

MDPI

Article

Ultrasound-Assisted Melt Extrusion of Polymers with the Main Harmonics of 10–60 kHz

Diana Agüero-Valdez, Alain González-Sánchez, María Teresa Rodríguez-Hernández, Heidi Andrea Fonseca-Florido, Juan Guillermo Martínez-Colunga, Janett Anaid Valdez-Garza, Gilberto Francisco Hurtado-López, Víctor Javier Cruz-Delgado * and Carlos Alberto Ávila-Orta *

Centro de Investigación en Química Aplicada, Enrique Reyna Hermosillo No. 140, Col. San José de los Cerritos, Saltillo 25294, Mexico; dian-av@hotmail.com (D.A.-V.); alain.glez.sse@gmail.com (A.G.-S.); teresa.rodriguez@ciqa.edu.mx (M.T.R.-H.); heidi.fonseca@ciqa.edu.mx (H.A.F.-F.); guillermo.martinez@ciqa.edu.mx (J.G.M.-C.); janett.valdez@ciqa.edu.mx (J.A.V.-G.); gilberto.hurtado@ciqa.edu.mx (G.F.H.-L.)

* Correspondence: victor.cruz@ciqa.edu.mx (V.J.C.-D.); carlos.avila@ciqa.edu.mx (C.A.Á.-O.); Tel.: +52-844-438-9830 (ext. 1391) (V.J.C.-D. & C.A.Á.-O.)

Abstract: Using a digital oscilloscope, the main harmonics resulting from the application of different frequencies and power levels of ultrasonic waves during the polymer extrusion process were identified. The primary harmonics are located between 10 and 60 kHz and exhibit unique characteristics, such as shape, crest, and trough, the latter being associated with voltage and current. The crest-to-trough distance (height) observed during processing at 34 kHz and 375 W shows the highest value, which correlates with the highest melt flow index and the lowest apparent viscosity. It is well known that the application of ultrasonic waves can randomly break C-C bonds in hydrocarbon compounds, leading to a decrease in molecular weight. However, the application of ultrasonic waves at different frequencies and power levels can promote chain scission in both high- and medium-molecular-weight polymer chains, thereby increasing the molecular weight distribution. This phenomenon can lead to chain disentanglement, along with chain scission, as evidenced by a decrease in molecular weight at medium power and frequency intensities. Finally, a schematic representation of the interaction between polymer chains and ultrasonic waves is proposed.

Keywords: ultrasonically assisted melt extrusion; polypropylene; monitoring; oscilloscope; harmonics

check for updates

Academic Editor: D. Andrew S. Rees

Received: 15 March 2025
Revised: 23 May 2025
Accepted: 1 June 2025
Published: 5 June 2025

Citation: Agüero-Valdez, D.; González-Sánchez, A.; Rodríguez-Hernández, M.T.; Fonseca-Florido, H.A.; Martínez-Colunga, J.G.; Valdez-Garza, J.A.; Hurtado-López, G.F.; Cruz-Delgado, V.J.; Ávila-Orta, C.A. Ultrasound-Assisted Melt Extrusion of Polymers with the Main Harmonics of 10–60 kHz. *Fluids* **2025**, *10*, 150. https://doi.org/10.3390/fluids10060150

Copyright: © 2025 by the authors. Licensee MDPI, Basel, Switzerland. This article is an open access article distributed under the terms and conditions of the Creative Commons Attribution (CC BY) license (https://creativecommons.org/licenses/by/4.0/).

1. Introduction

Ultrasonic waves are a type of wave that can propagate through different media (solid, liquid, or gas). These waves typically carry mechanical energy through the local vibration of particles without actually transporting the particles themselves. Ultrasound is generally defined as waves with frequencies above the upper limit of human hearing (typically considered to be 20 kHz) [1]. Ultrasonic waves have been widely employed across various disciplines, including biology, medicine, chemistry, physics, and materials science, because of their cost-effectiveness and environmentally friendly nature. This technology is commonly used in industrial applications and has been successfully tested in both laboratory and field conditions [2]. The effectiveness of ultrasonic waves in these processes is attributed to their ability to enhance heat and mass transfer, as well as modify the structure and properties of dispersed phases. This is achieved through the generation of mechanical energy, which is converted into acoustic waves that propagate through the medium, producing secondary effects.

One of the most significant effects of ultrasonic waves is the cavitation phenomenon, in which acoustic vibrations subject the liquid to high stress, leading to the formation of bubbles. The collapse of these bubbles results in the formation of a shock wave, which can significantly accelerate diffusion processes and increase localized heating [3]. Recently, Dengaev et al. [4] suggested that, in addition to cavitation and heating mechanisms, ultrasonic waves may also interact through other mechanisms, such as acoustic transmission and radiation forces. Acoustic transmission refers to the movement of fluid caused by the propagation of sound waves, which can enhance mixing and mass transfer. Radiation forces refer to the transfer of momentum from the sound wave to the medium, which can induce movement and separation of particles in viscous liquids such as crude oil.

Based on these principles, ultrasonic irradiation has been used for the synthesis of nanoparticles, like hydroxyapatite, graphene, and carbon nanomaterials [5–7]. Ultrasound-assisted methods have been used in *in-situ* emulsion polymerization for polymer nanocomposites, helping in the preparation of stable and finely dispersed polymer nanocomposites and developments in the preparation of core-shell particles [8,9], in addition to ultrasound-assisted adsorption of dyes on nanoparticles and composites [10] and water remediation [11,12]. Ultrasonic waves have also been employed as a nondestructive technique for assessing agricultural product quality, among other applications [13]. In engineering applications, ultrasonic waves have been used during the processing of molten polymers, a technique known as ultrasound-assisted melt extrusion (USME). The USME process has been employed to enhance polymer compatibility [14], improve the dispersion of nanoparticles in polymers [15,16], and promote the production of branched polymers [17]. However, the interaction mechanism between polymer chains and ultrasonic waves remains largely unexplored. In the USME process, an extruder, an adapter, a horn, and an ultrasonic generator are required. When the generator is connected to the power source, it converts low-frequency electrical energy into high-frequency energy. This energy is then transformed into mechanical vibrations through a piezoelectric transducer, which amplifies the signal and transfers the vibrational energy to the medium or material [18].

When propagating through a liquid or gaseous medium, ultrasonic waves are characterized as longitudinal waves, meaning that compression and rarefaction occur in the same direction as wave propagation [2]. Consequently, when the horn vibrates, it transfers energy to the media, which then propagates by the common modes, in addition to acoustic transmission and radiation forces [4]. Various techniques exist to measure the effects and efficiency of this process. However, the most commonly used methods involve post-processing evaluations of the material's physicochemical, rheological, thermal, electrical, or mechanical properties [15].

Since ultrasonic generators operate as an electrical circuit, it is possible to monitor voltage and current variations using an oscilloscope. An oscilloscope is an instrument used to visualize, measure, record, and analyze variations in voltage signals over time [19]. Kumar et al. [20] analyzed voltage and current signals using a high-speed digital oscilloscope to gain a deeper understanding of the arc welding process. They varied power sources, inverters, and welding electrodes, finding that oscilloscope data could differentiate the performance of various power sources and consumables in the welding process. A similar study was conducted by Savyasachi et al. [21], who monitored a metal arc welding process using different power sources and welding electrodes. Dynamic variations in current and voltage were recorded using a digital oscilloscope, while the arc welding process was recorded with a high-speed camera. The voltage and current data were analyzed using probability distribution analysis. These authors found that voltage variations could be correlated with physical processes. They demonstrated the feasibility of using an oscilloscope and a high-speed camera for supervising the arc welding process.

Most studies reported to date have focused on the application of ultrasonic waves generated at a single frequency within the range of 15–100 kHz, primarily at 20 ± 1 kHz, as this is the main or resonant frequency of commercial piezoelectric transducers and ultrasonic generators, as reported by Hamidi et al. [22]. For example, in the study by Mohammadian et al. [23], different frequencies (25, 40, and 65 kHz) were used, and the output power of the ultrasonic waves was varied between 50 and 500 W in each experiment. The effects on crude oil recovery were examined, identifying output power as the most significant factor. Increased output power (intensity) and higher wave frequencies resulted in enhanced and accelerated oil recovery. Specifically, ultrasonic waves increased oil recovery by 10%, 14%, and 17% for output power levels of 100, 200, and 400 W, respectively. Additionally, at an output power of 100 W, with a treatment time of 200 min, and at a frequency of 25 kHz, the recovery rate was 51%. In comparison, it reached 53% and 57% at frequencies of 40 kHz and 65 kHz, respectively. Recently, Dengaev et al. [24] demonstrated that using multi-frequency ultrasound facilitated a reduction in heavy crude oil viscosity by applying ultrasonic waves with principal harmonics between 20 and 60 kHz. They proposed that molecular degradation occurs when valence bond energy is lower than the external forces acting upon it. In normal alkanes, this effect is primarily observed in C-C bonds located near the center of the molecule, while in aromatic hydrocarbons with alkyl substituents, it occurs at the β-bond of peripheral chains.

To date, the effects observed upon the application of ultrasonic waves to molten polymers have been explained by cavitation collapse, which reduces the non-Newtonian flow characteristics of the molten polymer [25] or the formation of microvoids within the material due to cavitation during extrusion [26]. However, some research groups have proposed alternative mechanisms based on molecular segment relaxation and fatigue effects caused by successive expansion and compression cycles in polymer chains [27–29].

Given these considerations, the novelty of this work lies in studying the ultrasound-assisted melt extrusion process under the application of main harmonics and establishing correlations between electrical parameters (voltage, current, frequency, power) and the final physicochemical properties.

2. Materials and Methods

2.1. Materials

A polypropylene homopolymer (iPP) designed for cable coating applications and nonwoven fabric manufacturing, with a melt flow index of 35 g/10 min, was used. The material was obtained from Formosa Plastics Corporation (Point Comfort, TX, USA) under the commercial name Formolene 4111T.

2.2. Sample Preparation

The iPP was processed in a PRISM TSE 24-MC twin-screw extruder from Thermo Fisher Scientific (Karlsruhe, Germany), with a configuration of two high shear zones at a speed of 100 rpm and a flat temperature profile of 200 °C along the barrel. A specially designed chamber containing a catenoidal titanium horn from Branson Ultrasonics Corp. (Brookfield, CT, USA), with a primary frequency of 20 ± 0.1 kHz, was used for the ultrasonic treatment. The horn had a diameter of 0.5 inches and a total length of 3 1/2 inches, with 2 inches of straight cross-sectional length and a 0.5-inch exponential section. The horn was connected to the extruder die via a threaded joint in the direction of polymer flow.

The chamber consisted of a hollow steel cylinder threaded at both ends, with a total length of 5.2 inches. One end was connected to the extruder die via another hollow threaded cylinder (1/4-inch internal diameter) in the direction of polymer flow. At the opposite end, the horn was attached via a threaded joint (1 1/2-inch diameter). This chamber had a

controlled temperature and a nozzle for material output. The gap between the cross-section of the horn and the chamber was 0.25 inches, while the gap between the nozzle and the horn was 1 inch, located at the end of the exponential section. The horn was secured to the chamber via a countercurrent threaded connection to the polymer exit. A detailed drawing of this device can be found in Supplementary Material Figure S1.

The horn was connected to a piezoelectric transducer model CL33, from QSonica Sonicators Inc. (Newtown, CT, USA), by screwing it at its nodal point. The transducer was then connected to a homemade ultrasonic generator, operating within a frequency range of 10 to 60 kHz (adjustable via a tuning knob), with a maximum output power of 750 W. The generator included an impedance-matching circuit and a suppression circuit to protect it from parasitic frequencies. This system compensated for return voltage fluctuations due to rebound vibrations when the horn tip made contact with the molten polymer. This protection ensured the proper operation of the system and was reported elsewhere [15,30].

To analyze the behavior of ultrasonic waves, an Agilent DSO3102A digital oscilloscope, now Keysight (Santa Rosa, CA, USA), was connected to the ultrasonic generator and a PC running Windows™ XP. The oscilloscope software (Series 3000, version 1.1.27) was used to visualize and record ultrasonic wave signals at different frequencies and power levels. Figure 1 presents a schematic representation of the system used in this study.

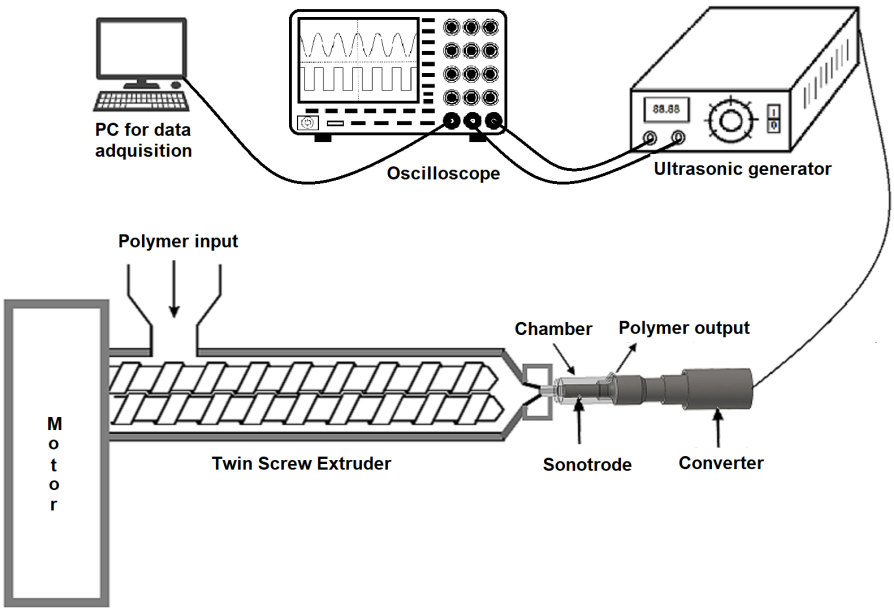

Figure 1. Schematic representation of the ultrasound-assisted melt extrusion process and oscillogram capture.

2.3. Characterization Techniques

A physicochemical characterization was conducted using various techniques to determine the effect of ultrasound variables, such as voltage, current, frequency, and power, after iPP processing via USME.

2.3.1. Oscillograms

An Agilent Technologies DSO3102A oscilloscope with a bandwidth of 100 MHz, a maximum sampling rate of 1 GS/s, two channels, and AC/DC coupling was used to record in situ ultrasonic waves. The device featured a 5.7-inch graphical display with an input impedance of 1 MΩ. A probe was used to measure voltage and current, with measurements obtained directly from the probes connected to the oscilloscope. During the USME process, the system's natural harmonics were identified, and the voltage and current

of the entire circuit were monitored to detect changes due to variations in ultrasonic power and frequency. Data were visualized and collected via an external PC connected through an Ethernet cable, with subsequent analysis conducted using the proprietary software of the oscilloscope.

2.3.2. Molecular Weight Analysis

The number-average molecular weight (Mn) and molecular weight distribution (Mw/Mn) of the ultrasonic-treated samples were determined using a gel permeation chromatography (GPC) system Alliance GPCV-2000, now Waters Corporation (Milford, MA, USA), with a refractive index detector. Trichlorobenzene was used as the mobile phase solvent. The analysis was conducted at a temperature of 140 °C, and the GPC was calibrated using polystyrene standards.

2.3.3. Melt Flow Index (MFI)

The melt flow index of the ultrasonic-treated samples was determined using a plastometer model LMI Series 4000 from Dynisco (Franklin, MA, USA) under a load of 2.16 kg at 230 °C, following ASTM D1238 [31].

2.3.4. Capillary Rheometry

The effect of ultrasonic waves on molecular mobility and viscosity was analyzed using a high-pressure capillary rheometer, Goettfert Rheograph 25 (Buchen, Germany), equipped with a die and a 15 mm diameter piston. The analysis was performed at 230 °C, with a shear rate range of 12 to 4800 s^{-1}. This shear rate range encompasses various polymer processing methods, including compression molding, extrusion, and injection molding, as specified in ASTM D3835 [32].

3. Results

3.1. Collection of Oscillograms

In this study, "harmonics" are defined as those frequencies that exhibit a stable waveform and can be consistently replicated in a digital oscilloscope. These harmonics were identified based on minimal noise and interference in the voltage and current signals, as well as their attenuation or magnification. The observed alterations in electrical behavior originate from the mechanical stress applied by the molten polymer on the horn tip, leveraging the well-known property known as the piezoelectric effect [17,18]. In this scenario, the polymer acts as a resistive element, generating electric charges in response to the applied pressure. Consequently, variations in polymer viscosity induced by ultrasonic wave exposure result in corresponding modifications in both current and voltage. As a result, a characteristic waveform pattern is observed for each voltage–current pair at each of the detected harmonics [20,24]. It is essential to clarify that while the horn is designed to resonate at a primary frequency of 20 kHz, this is determined when it is not immersed in a fluid. However, when the horn is in contact with a fluid, the resonance frequencies are modified due to changes in the density or viscosity of the medium, reducing the probability of cavitation [1].

The electrical system operates by converting conventional low-frequency electrical energy (60 Hz) into ultrasonic energy (10–100 kHz) using an ultrasonic generator. This high-frequency energy is subsequently transferred to the piezoelectric transducer. Through the expansion and contraction of metallic electrodes connected to the piezoelectric elements, the transducer generates longitudinal mechanical vibrations that are ultimately transmitted directly to the polymer as a shock wave front. These generated vibrations exhibit a periodic

oscillatory behavior governed by the applied voltages and currents, which are determined by the frequency and power supplied by the generator.

To monitor the electrical behavior of the system and detect changes induced by the piezoelectric effect, an oscilloscope was connected to the voltage and current outputs of the ultrasonic generator. The oscilloscope recorded sinusoidal oscillations of voltage and current as "oscillograms", providing an instantaneous and non-invasive representation of these signals, as illustrated in Figure 2. In addition to the variations in voltage–current parameters, the observed behavior also exhibited a certain degree of phase shift, meaning a forward or backward delay in the current signal relative to the voltage signal [20]. These changes in electrical parameters and phase shift are unique system behaviors that were quantified and analyzed.

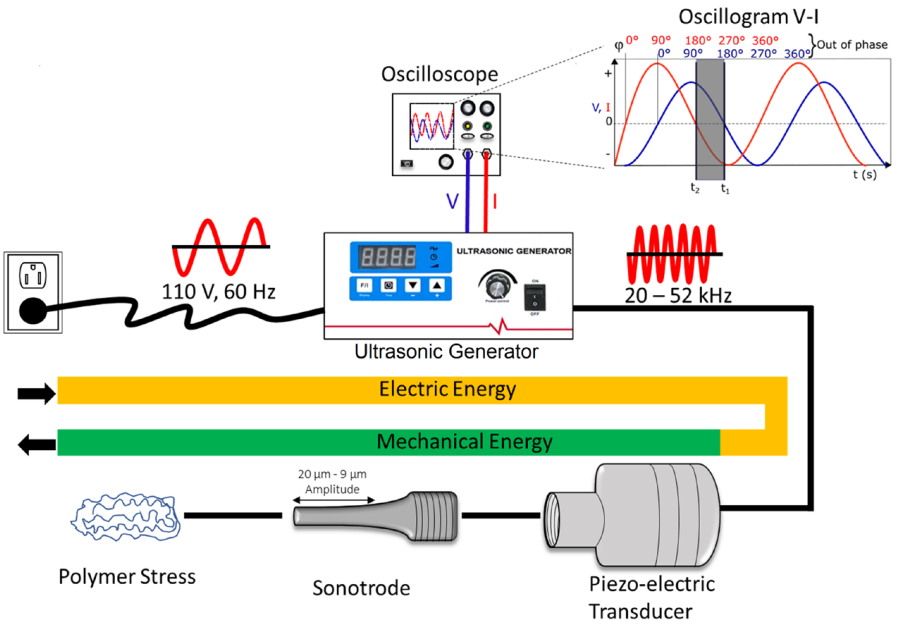

Figure 2. Schematic representation of the energy change in the system from electric to mechanical and interaction with the polymer.

Based on these observations, different harmonics were identified at 20, 25, 27, 34, 43, and 52 ± 0.1 kHz for working power levels of 225, 375, and 450 W. Under these conditions, it was found that beyond 450 W, no frequency exhibited stable signals. The samples were labeled accordingly. The W_U sample refers to polypropylene extruded without ultrasound, while ultrasound-treated extruded samples are labeled with the corresponding frequency and power used.

The voltage and current output signals were analyzed for each condition pair (frequency–power) (Figure 3). It was observed that increasing power at a constant frequency increased both voltage and current values, with the current signal exhibiting a positive shift relative to the voltage. At low frequencies (20, 25, and 27 kHz) and power levels exceeding 375 W, the current wave presented more significant interference in the system, with its amplitude failing to remain constant. Conversely, at frequencies above 27 kHz, the voltage and current waves exhibited a more defined waveform. The maximum peak values (crest), known as maximum amplitude (Amax), represent the amount of energy transmitted to the molten polymer, serving as a valuable indicator of material behavior. Table 1 presents the parameters, such as period (T) and maximum amplitude (Amax), associated with each voltage and current wave. The amplitude values of voltage and current increased as the power increased. At frequencies of 20 and 43 kHz, the current wave exhibited a phase shift relative to the voltage wave, indicating greater charge accumulation in the horn. However,

at a frequency of 34 kHz, the voltage values were lower, while the current values were higher than at any other frequency under the same applied power. Additionally, the voltage and current waves were observed to be in phase. Interferences or deviations from the characteristic sinusoidal behavior of an electrical voltage and current wave were primarily attributed to variations in polymer viscosity, which caused higher or lower pressure on the horn, modifying the electrical charge and work required for the horn to operate at a specific amplitude at a given frequency [20].

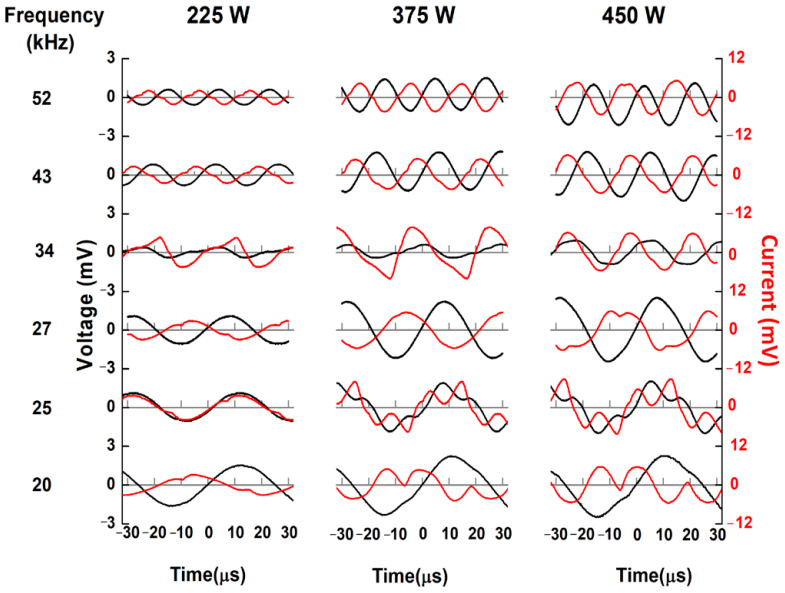

Figure 3. Oscillograms obtained from ultrasonic waves applied under different conditions.

Table 1. Values of the period, voltage, maximum current, and phase shift under different conditions.

Power (W)	Frequency (kHz)	Period (s)	V_{max} (mV)	I_{max} (mV)	Phase Shift (°)
W_U	-	-	-	-	-
225	20	5.0×10^{-5}	1.6	3.2	133
	25	4.0×10^{-5}	1.2	3.8	0
	27	3.7×10^{-5}	1.2	3.0	144
	34	2.9×10^{-5}	0.5	4.6	75
	43	2.3×10^{-5}	0.8	2.6	121
	52	1.9×10^{-5}	0.7	2.2	151
375	20	5.0×10^{-5}	2.2	5.0	132
	25	4.0×10^{-5}	2.0	8.2	29
	27	3.7×10^{-5}	2.2	5.5	139
	34	2.9×10^{-5}	1.2	7.8	13
	43	2.3×10^{-5}	1.6	4.7	108
	52	1.9×10^{-5}	1.8	4.5	180
450	20	5.0×10^{-5}	2.4	5.6	134
	25	4.0×10^{-5}	2.0	8.8	35
	27	3.7×10^{-5}	2.5	5.9	139
	34	2.9×10^{-5}	0.9	11.6	2
	43	2.3×10^{-5}	1.9	6.3	114
	52	1.9×10^{-5}	1.4	5.4	155

3.2. Molecular Weight Analysis

A molecular weight analysis was conducted to understand the effect of ultrasonic waves (frequency and power) on the molecular weight of iPP chains. Figure 4 shows the molecular weight distribution curves for the samples processed with and without ultrasound under different conditions. Detailed molecular weight values are provided in Table 2. The GPC traces shifted to lower values compared to the untreated sample, regardless of the applied power, indicating a reduction in molecular weight as the curves moved toward lower molecular weights. Overall, both Mw and Mn decreased upon ultrasound application. However, the number-average molecular weight (Mn) decreased more significantly than the weight-average molecular weight (Mw). This effect was most pronounced at a frequency of 34 kHz and a power of 375 W. Additionally, a decrease in peak amplitude was observed for the ultrasound-treated samples, indicating that chain scission occurred randomly, favoring the cleavage of high- and medium-molecular-weight chains, increasing the molecular weight distribution, and reducing Mw. This suggests that greater polymer chain scission was induced after ultrasonic treatment, consistent with the literature reports [25,29].

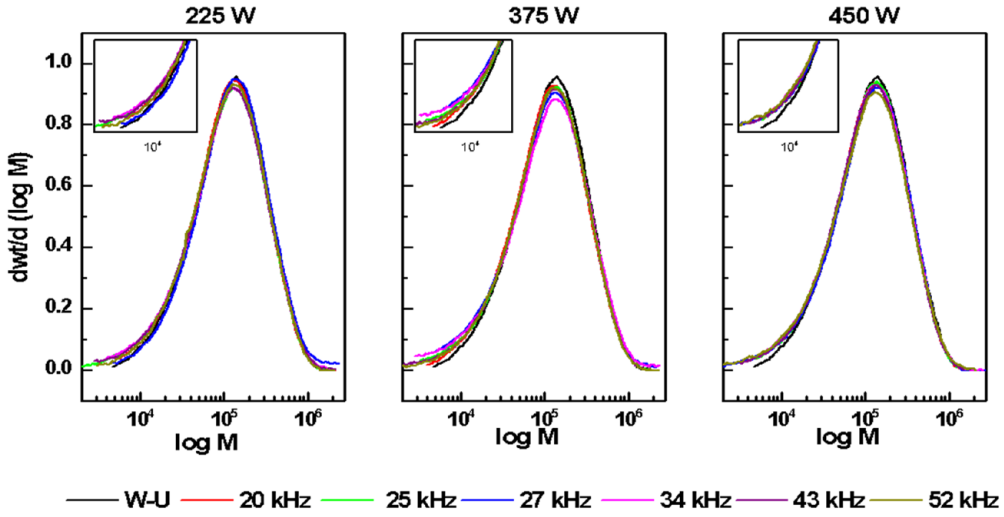

Figure 4. GPC traces of extruded samples under different conditions.

Table 2. Molecular weight of the samples processed under different conditions.

Power (W)	Frequency (kHz)	Mw × 10^{-4} (g/g-mol)	Mn × 10^{-4} (g/g-mol)	Mw/Mn (Dimensionless)
W_U	-	17.48	6.70	2.6
225	20	16.80	6.34	2.6
	25	16.58	5.10	3.2
	27	17.06	6.01	2.8
	34	16.98	5.62	3.0
	43	16.84	5.33	3.2
	52	16.72	5.83	2.9
375	20	17.16	5.97	2.9
	25	16.82	5.45	3.1
	27	17.57	5.71	3.1
	34	17.84	4.86	3.7
	43	16.68	5.01	3.3
	52	16.70	5.26	3.2

Table 2. *Cont.*

Power (W)	Frequency (kHz)	Mw × 10^{-4} (g/g-mol)	Mn × 10^{-4} (g/g-mol)	Mw/Mn (Dimensionless)
450	20	16.74	6.08	2.8
	25	16.76	5.97	2.8
	27	17.02	5.22	3.3
	34	17.00	6.35	2.7
	43	16.66	5.58	3.0
	52	16.86	4.91	3.4

3.3. Effect of Ultrasonic Waves on the MFI

The pure iPP exhibited an MFI value of 34 g/10 min, as measured in the laboratory and shown in Figure 5. Following polymer extrusion without ultrasonic treatment, an increase of 3 units in the MFI was observed compared to the pure iPP, attributed to the extrusion process itself. When ultrasonic waves were applied to the molten polymer, the increase in the MFI of the extruded iPP was found to be a function of both frequency and power, with values ranging from 38 to 41 g/10 min. Ultrasonic waves induce chain scission in iPP, allowing it to flow more efficiently than pure polypropylene and extruded iPP without ultrasound treatment. This behavior results from the combined effects of acoustic transmission and radiation forces. The highest MFI value was recorded at a power of 375 W and a frequency of 34 kHz, reaching 41 g/10 min. This observation is consistent with the GPC results, which indicate an increased polydispersity of the polymer chain.

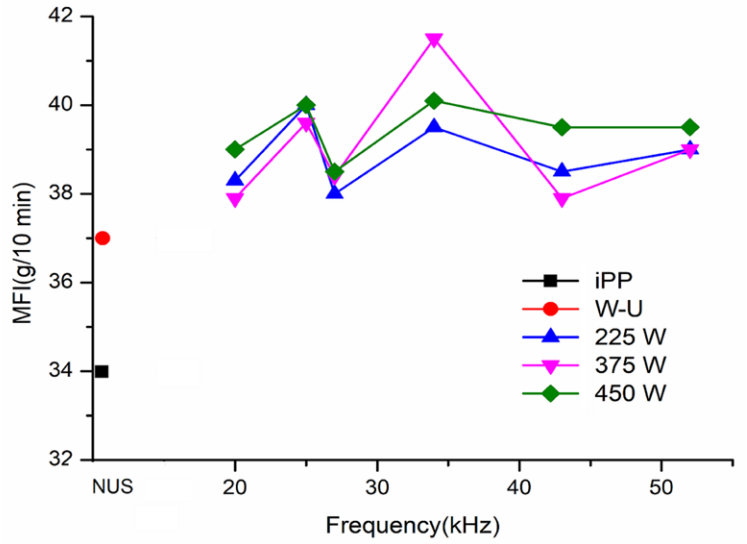

Figure 5. MFI values for samples processed under different conditions. Note, on the frequency axis, NUS means "non-ultrasonic treated".

A similar behavior was reported by Francucci et al. [33] in a polypropylene matrix subjected to ultrasonic treatment. The initial value of MFI was reported as 20 g/10 min. After applying different processing conditions, such as temperature, feed rate, and screw speed, the MFI values tended to increase or even undergo degradation at a temperature profile of 220 °C and higher speeds, including 750 and 1000 rpm. Meanwhile, with a temperature profile of 180 °C, the increase in the MFI values was lower, even at higher screw speeds. The effect of US irradiation was negligible up to an intensity power of 60%, and with the highest separation distance of the polymer–sonotrode.

3.4. Rheological Analysis

Capillary rheometry was used to evaluate the material's viscous behavior under deformation. Figure 6 illustrates the effect of ultrasonic waves on selected samples, including pure iPP, W_U, and samples treated at 34 kHz and different power levels.

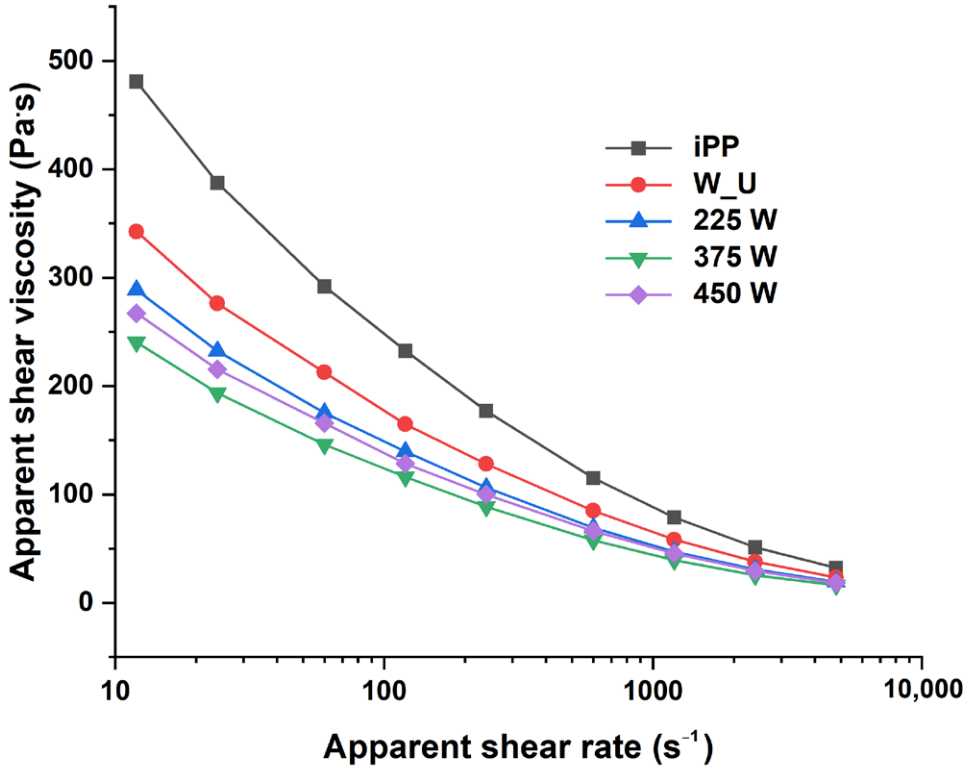

Figure 6. Capillary rheometry for samples processed under different conditions.

In general, as the apparent shear stress increases, the apparent viscosity of the materials gradually decreases. The highest viscosity value was observed in the pure iPP, followed by the W_U sample, both of which are consistent with values reported in the literature [34]. When ultrasonic waves were applied at 34 kHz, the apparent shear viscosity exhibited a greater reduction than in the W_U sample, particularly at power levels of 225 and 450 W. However, the sample treated at 375 W exhibited the most significant decrease in apparent shear viscosity, attributed to molecular weight reduction and chain scission during processing. This increase in polymer fluidity during extrusion may offer several advantages, including higher production rates, improved extrudate quality, and the formation of a beta phase during polymer crystallization [35].

3.5. Polymer Chain Interactions and Ultrasonic Wave Model

Figure 7 presents a conceptual model illustrating the potential effects of ultrasonically assisted melt extrusion on polymer chains. It is well established that polymers undergo orientation and stress due to extensional flow during the extrusion process, resulting in various conformations of the polymer chain. Upon exiting the die, the chains rapidly interact with ultrasonic waves due to acoustic transmission and radiation forces, which collectively influence the final orientation and structure. Since longer polymer chains have higher relaxation times than shorter chains, greater interchain friction is expected, reducing the number of entanglements (Figure 7a). Other chains undergo stretching and disentanglement (Figure 7b,c), followed by polymer chain scission (Figure 7d,e).

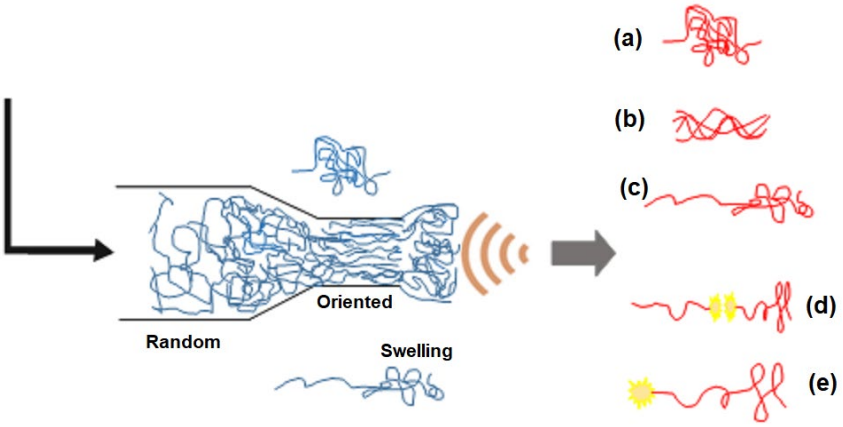

Figure 7. Diagram of the proposed mechanism of the effect of ultrasonic waves during the ultrasound-assisted melt extrusion process. (**a**) entangled polymer chain, (**b**) stretched polymer chain, (**c**) disentangled polymer chain, (**d**) polymer middle-chain scission, and (**e**) polymer end-chain scission.

4. Discussion

The piezoelectric transducer undergoes mechanical deformation due to the vibrations generated by the ultrasonic generator when employing different natural harmonics of the system, resulting in variations in voltage and current. The oscilloscope enables the analysis of the waveform of these signals, including amplitude, frequency, phase, and other relevant characteristics. Consequently, the oscilloscope provides precise information regarding electrical changes associated with the piezoelectric effect, enabling real-time, in situ monitoring and analysis of system behavior.

When ultrasonic waves interact with polymer chains, they can generate vibratory motion known as acoustic transmission, inducing a "stretching and relaxation" effect. This can lead to greater friction between chains, promoting chain disentanglement and polymer chain scission. It has been widely reported that one of the most notable effects of ultrasonic waves is the reduction of molecular weight. Chen et al. [27] investigated the physical and chemical effects of ultrasound on polypropylene matrices at an operational frequency of 20 kHz. Their findings indicated that as ultrasonic power increased (0–200 W), a reduction in molecular weight and molecular weight distribution of polypropylene was observed.

Ultrasonic waves can create chain scission points due to acoustic transmission and radiation forces, as observed in heavy oil crude and lower-molecular-weight hydrocarbons [4,22–24], leading to chain fragmentation and enhanced material fluidity. This finding aligns with various reports in the literature, which show that the application of ultrasonic waves to a polypropylene matrix during extrusion leads to a reduction in die pressure and apparent viscosity, as well as increased production rates, reduced extrudate swelling, and improved surface quality of the extruded PP [16,25,26,29,33,35].

As demonstrated, reductions in molecular weight and increases in polymer fluidity are significantly influenced by ultrasonic waves, depending on the applied frequency and power. This observation supports the hypothesis that each harmonic interacts with polymer chain segments of a similar size, promoting chemical reactions and secondary effects that enhance the processability of polymers.

Depending on the structure and nature of the polymer, the mechanical energy supplied by ultrasonic waves may also influence polymer reactivity. Based on the voltage and current oscillograms, the polymer exhibits distinct harmonics between 10 and 60 kHz, suggesting that each specific frequency–power combination of ultrasonic waves may induce different effects on the polymer chain. Given these findings, further research is warranted on other polymers with different chemical structures and in the presence of functional additives to explore their response to ultrasonic waves.

5. Conclusions

For the first time, the primary harmonics between 10 and 60 kHz were identified in a single ultrasonic generator/converter/sonotrode system with the aid of an oscilloscope. Ultrasonically assisted polypropylene extrusion was performed using the identified harmonics. Applying ultrasonic waves during polymer extrusion increases the vibrational energy of polymer chains, primarily due to acoustic transmission and radiation forces, leading to polymer chain scission. This results in a reduction in molecular weight, an increase in melt flow index, and a decrease in viscosity. The 34 kHz frequency and 375 W power level exhibited the most effective coupling between voltage and current signals and induced the most significant modifications in the final properties of the polymer.

This study demonstrates that the effects of frequency and power on each identified harmonic improve polymer processability, suggesting potential applications for further studies on molecular weight, copolymer presence, and nanoparticle incorporation. Such investigations could aid in establishing a harmonic database to promote and optimize ultrasonic processing in polymer engineering.

Finally, the findings indicate that ultrasound-assisted extrusion can be monitored in real-time and non-invasively using a digital oscilloscope, enabling the identification of process-relevant electrical signals (oscillograms).

Supplementary Materials: The following supporting information can be downloaded at https://www.mdpi.com/article/10.3390/fluids10060150/s1: Figure S1: Detailed view of the device for ultrasonic treatment. Dimensions are in mm.

Author Contributions: Conceptualization, V.J.C.-D. and C.A.Á.-O.; methodology, D.A.-V. and A.G.-S.; software, G.F.H.-L.; validation, H.A.F.-F. and J.G.M.-C.; formal analysis, M.T.R.-H.; investigation, D.A.-V., J.A.V.-G. and A.G.-S.; writing—original draft preparation, D.A.-V. and A.G.-S.; writing—review and editing, V.J.C.-D. and C.A.Á.-O.; supervision, H.A.F.-F. and J.G.M.-C.; project administration, J.A.V.-G. All authors have read and agreed to the published version of the manuscript.

Funding: CONACYT Project TLAX-2018-01-01-43129.

Data Availability Statement: The data are contained within this article.

Acknowledgments: The authors acknowledge the financial support from CONACYT through TLAX-2018-01-01-43129 and the Secretaría de Ciencia, Humanidades, Tecnología e Innovación de México (SECIHTI) through scholarship 276952 for Diana Agüero-Valdez. The authors also extend their gratitude to Rubén Sierra-Ávila, María G. Méndez-Padilla, and Javier Gudiño-Rivera for their support in the experimental measurements conducted in this study.

Conflicts of Interest: The authors declare no conflicts of interest.

References

1. Leighton, T.G. What is ultrasound? *Prog. Biophys. Mol. Biol.* **2007**, *93*, 3–83. [CrossRef] [PubMed]
2. Saha, A.; Mathur, M. Ultrasound Physics & Overview. In *Ultrasound Fundamentals*; Springer International Publishing: Cham, Switzerland, 2021; pp. 3–16.
3. Ensminger, D.; Bond, L.J. *Ultrasonics*; CRC Press: Boca Raton, FL, USA, 2023; ISBN 9780429286964.
4. Dengaev, A.V.; Khelkhal, M.A.; Getalov, A.A.; Baimukhametov, G.F.; Kayumov, A.A.; Vakhin, A.V.; Gafurov, M.R. Innovations in Oil Processing: Chemical Transformation of Oil Components through Ultrasound Assistance. *Fluids* **2023**, *8*, 108. [CrossRef]
5. Poinern, G.E.; Brundavanam, R.K.; Mondinos, N.; Jiang, Z.-T. Synthesis and characterisation of nanohydroxyapatite using an ultrasound assisted method. *Ultrason. Sonochem.* **2009**, *16*, 469–474. [CrossRef] [PubMed]
6. Muthoosamy, K.; Manickam, S. State of the art and recent advances in the ultrasound-assisted synthesis, exfoliation and functionalization of graphene derivatives. *Ultrason. Sonochem.* **2017**, *39*, 478–493. [CrossRef]
7. Krishnaveni, M.; Asiri, A.M.; Anandan, S. Ultrasound-assisted synthesis of unzipped multiwalled carbon nanotubes/titanium dioxide nanocomposite as a promising next-generation energy storage material. *Ultrason. Sonochem.* **2020**, *66*, 105105. [CrossRef]

8. Bhanvase, B.A.; Sonawane, S.H. Ultrasound assisted in situ emulsion polymerization for polymer nanocomposite: A review. *Chem. Eng. Process. Process Intensif.* **2014**, *85*, 86–107. [CrossRef]
9. Soman, V.; Vishwakarma, K.; Poddar, M.K. Ultrasound assisted synthesis of polymer nanocomposites: A review. *J. Polym. Res.* **2023**, *30*, 406. [CrossRef]
10. Bagheri, A.R.; Ghaedi, M.; Asfaram, A.; Jannesar, R.; Goudarzi, A. Design and construction of nanoscale material for ultrasonic assisted adsorption of dyes: Application of derivative spectrophotometry and experimental design methodology. *Ultrason. Sonochem.* **2017**, *35*, 112–123. [CrossRef]
11. Zorgani, M.A.; Zaoui, F.; Zorgani, R.N.E.H.; Elhadj Daouadji, B.; Sebba, F.Z.; Choukchou-Braham, E.; Bounaceur, B.; Ma, Y.; Bhardwaj, M.; Ma, H. Ultrasonic-assisted adsorption of heavy copper and lead metal ions by g-C3N4, application of g-C3N4@MNPs (M: Pb, Cu) in the catalytic photoreduction of organic pollutants. *J. Water Process Eng.* **2024**, *58*, 104724. [CrossRef]
12. Zaoui, F.; Sebba, F.Z.; Liras, M.; Sebti, H.; Hachemaoui, M.; Mokhtar, A.; Beldjilali, M.; Bounaceur, B.; Boukoussa, B. Ultrasonic preparation of a new composite poly(GMA)@Ru/TiO_2@Fe_3O_4: Application in the catalytic reduction of organic pollutants. *Mater. Chem. Phys.* **2021**, *260*, 124146. [CrossRef]
13. Kim, K.-B.; Lee, S.; Kim, M.-S.; Cho, B.-K. Determination of apple firmness by nondestructive ultrasonic measurement. *Postharvest Biol. Technol.* **2009**, *52*, 44–48. [CrossRef]
14. Gunes, K.; Isayev, A.I.; Li, X.; Wesdemiotis, C. Fast in situ copolymerization of PET/PEN blends by ultrasonically-aided extrusion. *Polymer* **2010**, *51*, 1071–1081. [CrossRef]
15. Mata-Padilla, J.M.; Ávila-Orta, C.A.; Medellín-Rodríguez, F.J.; Hernández-Hernández, E.; Jiménez-Barrera, R.M.; Crúz-Delgado, V.J.; Valdéz-Garza, J.; Solís-Rosales, S.G.; Torres-Martínez, A.; Lozano-Estrada, M.; et al. Structural and morphological studies on the deformation behavior of polypropylene/multi-walled carbon nanotubes nanocomposites prepared through ultrasound-assisted melt extrusion process. *J. Polym. Sci. Part B Polym. Phys.* **2015**, *53*, 475–491. [CrossRef]
16. Isayev, A.I.; Jung, C.; Gunes, K.; Kumar, R. Ultrasound assisted single screw extrusion process for dispersion of carbon nanofibers in polymers. *Int. Polym. Process.* **2008**, *23*, 395–405. [CrossRef]
17. Kim, K.Y.; Nam, G.J.; Lee, J.W. Continuous extrusion of long-chain-branched polypropylene/clay nanocomposites with high-intensity ultrasonic waves. *Compos. Interfaces* **2007**, *14*, 533–544. [CrossRef]
18. Gallego-Juárez, J.A. Power ultrasonics: New technologies and applications for fluid processing. In *Ultrasonic Transducers*; Elsevier: Amsterdam, The Netherlands, 2012; pp. 476–516.
19. Dias Pereira, J.M. The history and technology of oscilloscopes. *IEEE Instrum. Meas. Mag.* **2006**, *9*, 27–35. [CrossRef]
20. Kumar, V.; Chandrasekhar, N.; Albert, S.K.; Jayapandian, J. Analysis of arc welding process using Digital Storage Oscilloscope. *Measurement* **2016**, *81*, 1–12. [CrossRef]
21. Savyasachi, N.; Chandrasekar, N.; Albert, S.K.; Surendranathan, A.O. Evaluation of Arc Welding Process Using Digital Storage Oscilloscope and High Speed Camera. *Indian Weld. J.* **2015**, *48*, 35. [CrossRef]
22. Hamidi, H.; Sharifi Haddad, A.; Wisdom Otumudia, E.; Rafati, R.; Mohammadian, E.; Azdarpour, A.; Giles Pilcher, W.; Wilhelm Fuehrmann, P.; Ricardo Sosa, L.; Cota, N.; et al. Recent applications of ultrasonic waves in improved oil recovery: A review of techniques and results. *Ultrasonics* **2021**, *110*, 106288. [CrossRef]
23. Mohammadian, E.; Parak, M.; Babakhani, P. The Effects of Properties of Waves on the Recovery of Ultrasonic Stimulated Waterflooding. *Pet. Sci. Technol.* **2014**, *32*, 1000–1008. [CrossRef]
24. Dengaev, A.V.; Kayumov, A.A.; Getalov, A.A.; Aliev, F.A.; Baimukhametov, G.F.; Sargin, B.V.; Maksimenko, A.F.; Vakhin, A.V. Chemical Viscosity Reduction of Heavy Oil by Multi-Frequency Ultrasonic Waves with the Main Harmonics of 20–60 kHz. *Fluids* **2023**, *8*, 136. [CrossRef]
25. Chen, J.; Chen, Y.; Li, H.; Lai, S.-Y.; Jow, J. Physical and chemical effects of ultrasound vibration on polymer melt in extrusion. *Ultrason. Sonochem.* **2010**, *17*, 66–71. [CrossRef] [PubMed]
26. Zhong, J.; Isayev, A.I.; Huang, K.Y. Influence of ultrasonic treatment in PP/CNT composites using masterbatch dilution method. *Polymer* **2014**, *55*, 1745–1755. [CrossRef]
27. Li, Y.; Li, J.; Guo, S.; Li, H. Mechanochemical degradation kinetics of high-density polyethylene melt and its mechanism in the presence of ultrasonic irradiation. *Ultrason. Sonochem.* **2005**, *12*, 183–189. [CrossRef]
28. Espinoza-Gonzalez, C.; Avila-Orta, C.; Martinez-Colunga, G.; Lionetto, F.; Maffezzoli, A. A Measure of CNTs Dispersion in Polymers With Branched Molecular Architectures by UDMA. *IEEE Trans. Nanotechnol.* **2016**, *15*, 731–737. [CrossRef]
29. Martínez-Colunga, J.G.; Cruz-Delgado, V.J.; Sánchez-Valdés, S.; Mata-Padilla, J.M.; Ramos-de Valle, L.F.; Espinoza-Martínez, A.B.; Benavides, R.; Ramírez-Vargas, E.; Rodriguez-Gonzalez, J.A.; Lara-Sanchez, J.F.; et al. Application of ultrasonic radiation for the development of polypropylene/multi-walled carbon nanotubes nanocomposites and its effect on the PP chemical degradation. *Iran. Polym. J.* **2024**, *33*, 1751–1764. [CrossRef]
30. Ávila Orta, C.A.; Martínez Colunga, J.G.; Bueno Baqués, D.; Raudry López, C.E.; Cruz Delgado, V.J.; González Morones, P.; Valdez Garza, J.A.; Esparza Juárez, M.E.; Espinoza González, C.J.; Rodríguez González, J.A. Proceso Continuo Asistido Por Ultrasonido

de Frecuencia y Amplitud Variable, Para la Preparación de Nanocompuestos a Base de Polímeros y Nanopartículas. MX Patent 323756, 19 September 2014.
31. *ASTM D1238-10*; Test Method for Melt Flow Rates of Thermoplastics by Extrusion Plastometer. ASTM: West Conshohocken, PA, USA, 2010. [CrossRef]
32. *ASTM D3835-16*; Test Method for Determination of Properties of Polymeric Materials by Means of a Capillary Rheometer. ASTM: West Conshohocken, PA, USA, 2016. [CrossRef]
33. Francucci, G.; Rodriguez, E.; Rodriguez, M.E. Ultrasound-Assisted Extrusion Compounding of Nano Clay/Polypropylene Nano Compounds. *Polymers* **2024**, *16*, 2426. [CrossRef]
34. Medellín Rodríguez, F.J.; Gudiño Rivera, J.; Rodríguez Velázquez, J.G.; Lara Sánchez, J.F.; Salinas Hernández, M. Gradually modified fibers of Yucca Filifera (Asparagaceae) as biodegradable and mechanical reinforcement of polypropylene composites. *Polym. Compos.* **2024**, *45*, 751–762. [CrossRef]
35. Lin, H.; Isayev, A.I. Ultrasonic treatment of polypropylene, polyamide 6, and their blends. *J. Appl. Polym. Sci.* **2006**, *102*, 2643–2653. [CrossRef]

Disclaimer/Publisher's Note: The statements, opinions and data contained in all publications are solely those of the individual author(s) and contributor(s) and not of MDPI and/or the editor(s). MDPI and/or the editor(s) disclaim responsibility for any injury to people or property resulting from any ideas, methods, instructions or products referred to in the content.